JOINT INSTITUTE FOR NUCLEAR RESEARCH

Dzelepov Laboratory of Nuclear Problems

FINAL REPORT ON THE START PROGRAM

Modeling a hypothetical Neutrino experiment at the long-range accelerator from Protvino to Baksan (PtB) in GNA software

---

Supervisor:
Kolupaeva Ludmila

Student:
Serga Sergey, Russia
Moscow State University

Participation period:
July 25 – August 16
Summer Session 2025

Dubna, 2025

Contents

Abstract

This report simulates a hypothetical accelerator neutrino experiment with a long base. The main work consists of calculating neutrino fluxes and cross sections, as well as estimating the annual number of events and the sensitivity of some oscillation parameters and neutrino mass hierarchy in the experiment using the GNA software.

1 Introduction

Modern neutrino experiments play a key role in studying the fundamental properties of neutrinos, their oscillations and interactions with matter. One of the promising directions is the use of accelerator neutrino beams, which make it possible to obtain intense and controlled particle fluxes for detailed studies. In this context, attention is drawn to a possible experimental setup linking the Protvino U-70 accelerator and the Baksan Underground Scintillation Telescope (BUST).

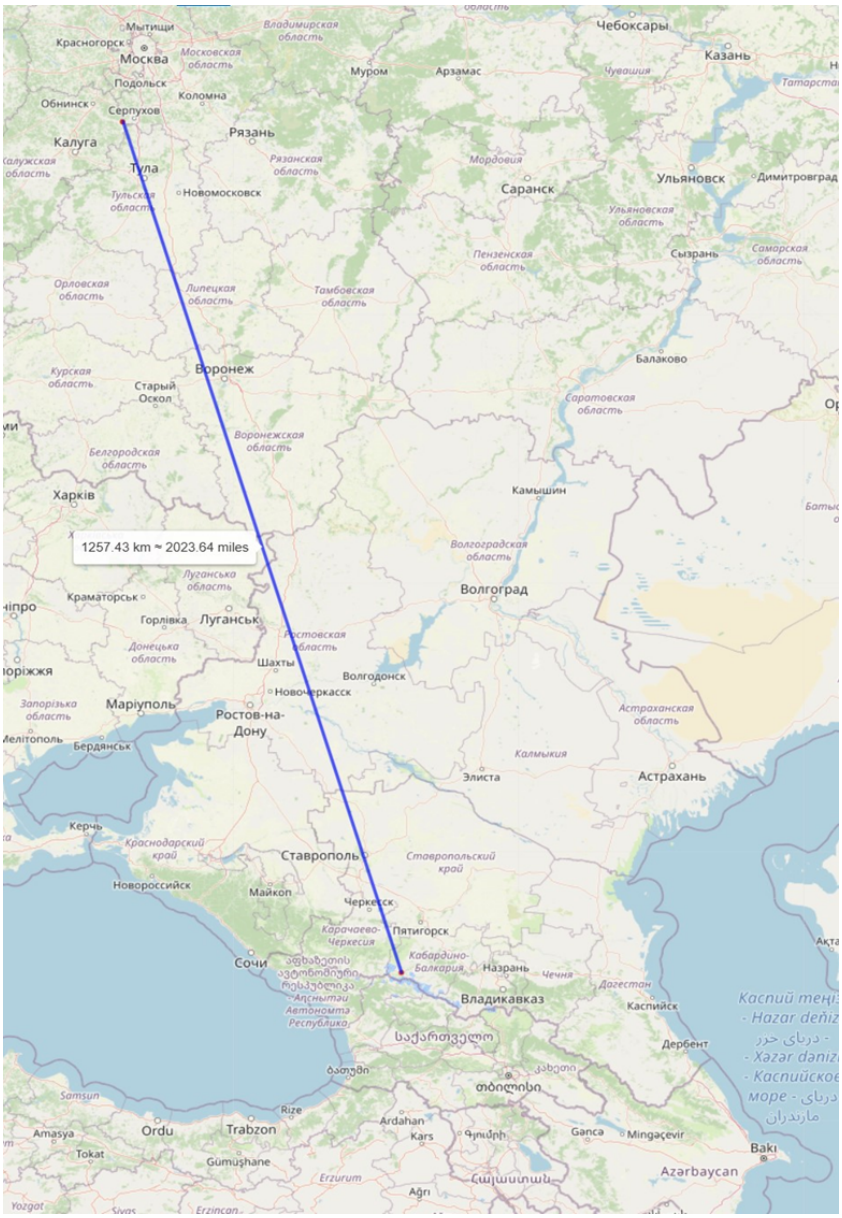

Figure 1: Geographical location of the accelerator (U-70) and detector (BUST).

The Protvino U-70 accelerator complex, located at the Institute of High Energy Physics (IFE, Protvino), is one of the largest in Russia and is capable of generating high-energy proton beams (up to 70 GeV) suitable for creating an intense neutrino beam. In turn, the Baksan Neutrino Observatory (INR RAS) has a unique infrastructure for detecting neutrinos, including an underground scintillation telescope protected from background cosmic particles by a mountain range.

Modeling of such an experiment requires taking into account many factors: the geometry of the beam, the generation of neutrinos, their propagation over a distance of about 1,350 km (Fig. 1) through the upper layers of the Earth, as well as the detection features in the BUST. Such calculations make it possible to estimate the expected neutrino flux, the sensitivity of the experiment to oscillatory measurements, and the potential for studying physical effects beyond the Standard Model.

This article discusses key aspects of modeling the U-70 $\rightarrow$ BUST accelerator neutrino experiment, including beam parameters, methods for calculating oscillations, and estimating the expected number of events in the detector. The results may be useful for planning future research in the field of neutrino and high-energy physics in Russia.

2 Accelerator and detector

Protvino Accelerator Complex (U-70)

U-70 is a proton synchrotron with an energy of 70 GeV, constructed in 1967 at the Institute for High Energy Physics, Protvino. At the time of its construction, the accelerator's energy was record-breaking, and it remains the highest-energy accelerator in Russia (54°52'15" N, 37°11'15" E).

Let us discuss the characteristics of the accelerator. The Protvino U-70 accelerator is a three-stage system, as follows:

1) Linear ion accelerator (LU400) at 400 MeV.
2) Fast-cycling proton synchrotron (U-3.5) at 3.5 GeV.
3) Main U-70 accelerator (70 GeV).

The proton energy reaches 70 GeV. At an approximately achievable operating power of 90 kW, the number of protons on target can be estimated as $N_p \approx 10^{20} \frac{\text{POT}}{\text{year}}$. At a cycle frequency of 1 pulse every 3 seconds.

In works [1] and [2], possible modifications to the U-70 accelerator complex are considered to increase the total power and, consequently, the number of POT per year. In the case of the maximum possible upgrade of the accelerator complex, the expected power will be ≈ 450 kW, and the maximum POT per year, which we will rely on, is 7.8×10^{20}.

Figures 2 and 3 present the upgraded design of the accelerator complex and options for directing the neutrino beam to various detectors.

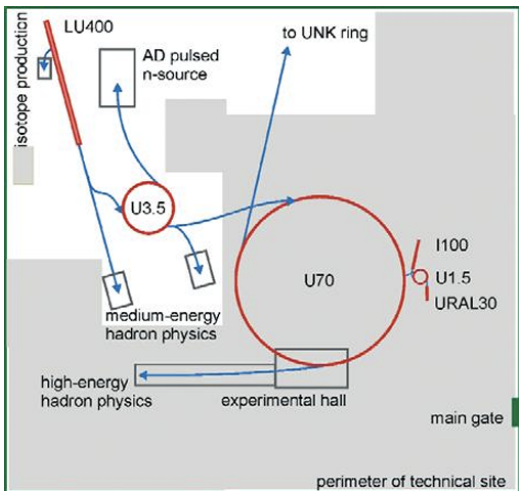

Figure 2: Schematic of the U-70 accelerator complex (considering the upgrade)[1].

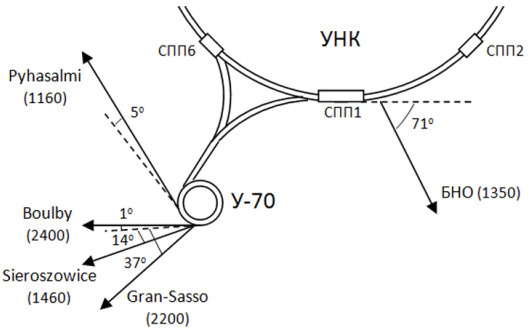

Figure 3: Options for directing the accelerated proton beam from the accelerator[1].

Neutrino Beam Parameters:

The broadband spectrum has a peak in the range of 2–4 GeV (for baselines of 1160–2200 km) [1]. From the spectra presented in Fig. 4, we are interested in the line "U70 (1350 km)". In the following, we will rely on this muon neutrino flux spectrum to determine the number of events registered in the detector.

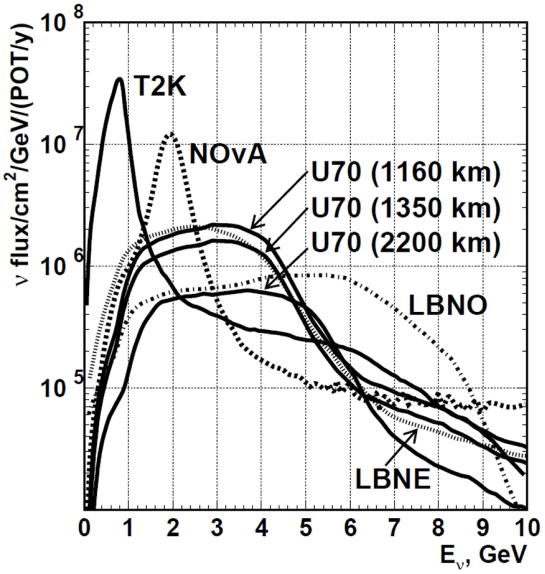

Figure 4: Energy spectra of muon neutrino fluxes without accounting for oscillations at detectors for various experiments [1].

Particles (pions/kaons) knocked out from the target are focused using magnetic horns and then decay into neutrinos with a selected direction of motion. The angular divergence can be estimated as the ratio $\theta \approx \frac{m_\pi}{T_\pi}$, since most pions produced in proton-nucleus collisions in the target have an emission direction aligned with the initial proton direction (Fig. 5).

Similar histograms can be observed for π^--mesons. Thus, the divergence angle of the initial beam can be approximately estimated as $\theta \approx 0.27$ rad at an average pion kinetic energy

of 2–3 GeV. This pion beam then enters the horn system, undergoing additional angular selection. By analogy with similar experiments, we assume that this system (Fig. 6) can provide a muon neutrino beam with $\theta \approx 0.01$ rad [3].

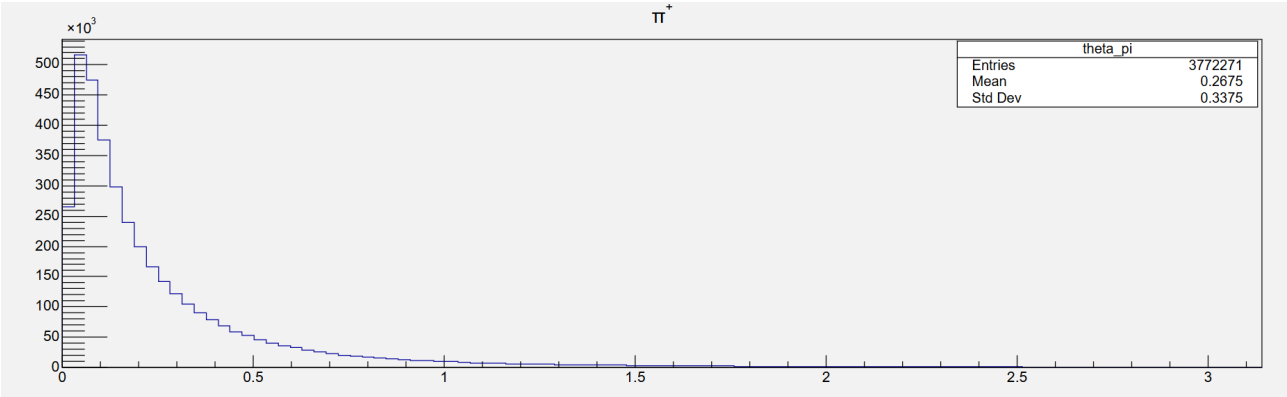

Figure 5: Angular distribution of π^+ at an incident proton energy of 70 GeV. The simulation was performed for a carbon target using the PYTHIA software.

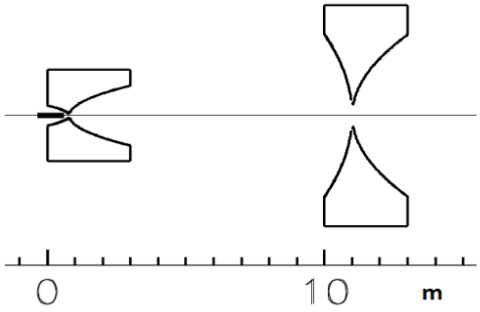

Figure 6: Focusing system for obtaining a narrowly directed neutrino beam [1].

In neutrino accelerator experiments, the focusing horn system, as mentioned above, ensures the formation of an intense and narrowly directed neutrino beam. Its primary task is to collect and focus secondary particles, predominantly pions and kaons, which subsequently decay, producing neutrinos.

Protons are accelerated to high energies and then directed onto a dense graphite target. As a result of proton-nucleus collisions in the target, secondary particles are produced—mainly charged pions (π^+, π^-) and kaons (K^+, K^0, K^-). These particles are emitted in various directions, and without additional focusing, a significant portion would be lost, leading to a reduction in the intensity of the final neutrino beam.

To address this issue, a magnetic horn system is used. The principle of operation is based on quadrupole magnets, which focus charged particles into a narrow beam. Our hypothetical configuration includes two horns: the first, called the collecting horn, captures particles emitted at large angles, while the second, the transfer horn, forms a parallel beam, directing it as needed.

After focusing, pions and kaons enter a dedicated decay volume long pipe filled with gas (helium in the NOvA and T2K experiments), where they decay in flight.

The main decay channels producing muon neutrinos are:

$\pi^+ \to \mu^+ + \nu_\mu$ (99.99 %)

$K^+ \to \mu^+ + \nu_\mu$ (63.56%)

$K^+ \to \pi^+ + \pi^0$ (20.67%)

These decay processes predominantly lead to the production of muon neutrinos; however, there are also channels producing electron neutrinos, and muon decays producing electron neutrinos should not be overlooked. In accelerator experiments like PtB, the majority of neutrinos in the initial flux are of the muon flavor. References [1] and [3] provide the following estimates:
$\nu_\mu/\bar{\nu}_\mu < 99$ %
$\nu_e/\bar{\nu}_e > 1$ %

Since neutrinos interact very weakly with matter, they continue moving in the same direction as the original pions, forming a narrowly directed beam. However, if the experiment includes a near detector, it is necessary to account for the presence of other particles in the beam, particularly muons produced from pion decays. To remove them, an absorber—a massive block of iron or another dense material—is placed in the beam's path. Muons, having significant mass, quickly lose energy and stop in the absorber, while neutrinos pass through freely, reaching the detector.

Baksan Underground Scintillation Telescope (BUST)

Basic information [4] about the detector at the Baksan Neutrino Observatory (BNO) (Baksan, Russia, baseline length - 1350 km, 43°16'32" N, 42°41'25" E):

Total number of detectors: 3180.

Total scintillator mass: 330 tons.

Effective detector area $S_{det} \simeq 400\,\mathrm{m}^2$

A standard module is an aluminum container with dimensions $(0.7 \times 0.7 \times 0.3)$ m^3, filled with a liquid scintillator based on white spirit with additives PPO (1 g/L) and POPOP (0.03 g/L). The inner surface is coated with white enamel, diffusely reflecting light.

Energy deposition measurements in individual detectors range from 0.05 to 1000 GeV.

Calculation of the Cross-Section for the PtB Neutrino Flux:

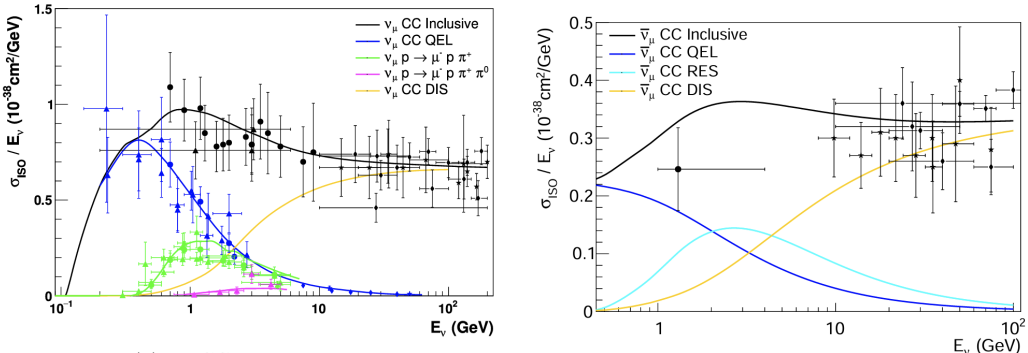

(a) ν_μ CC cross section.

(b) $\bar{\nu}_\mu$ CC cross section.

Figure 7: Approximations of experimental cross-section values in various energy ranges by interaction type are shown in different colors: blue - quasi-elastic scattering (QEL), green/cyan - resonance scattering (RES), yellow - deep inelastic scattering (DIS), black - total cross-section [5].

From Fig. 7, it is evident that the neutrino interaction cross-section with matter, divided by the neutrino energy, is nearly constant and, at our energies of approximately 3 GeV, equals: $0.85 * 10^{-38} \frac{\mathrm{cm}^2}{E_\nu \cdot \mathrm{nucleons}} \Rightarrow \sigma_\nu = 2.5 \times 10^{-38} \frac{\mathrm{cm}^2}{\mathrm{nucleons}}$.

Since the majority of the scintillator volume is occupied by white spirit, it is convenient, as a first approximation, to estimate the cross-section with the substance ($C_{10}H_{22}$). The total number of nucleons in one molecule is thus $N = 142$, hence:

$$\sigma_\nu = 3.55 \times 10^{-36}\,\text{cm}^2 \tag{1}$$

The total number of nucleons is $N_{nucl} = \frac{3.3\times10^8}{142} \times 6.022 \times 10^{23} \times 142 \approx 2 \times 10^{32}$.

3 Estimation of the Upper Bound on the Number of Events per Year

To estimate the number of neutrinos detected per year under ideal conditions, without accounting for oscillations and detector specifics:

$$n = \Phi_\nu * \sigma_\nu * N_{nucl}, \tag{2}$$

we first need to estimate the maximum value of the neutrino flux:

$$\Phi_\nu^{max} \sim \frac{N_p \times G \times k}{S_{det}}, \tag{3}$$

where G is a factor describing the geometry of the neutrino flux and the distribution of neutrinos within the beam (calculated in Section 2.1),
k is a coefficient reflecting the efficiency of neutrino production per proton in this experiment (based on estimates for similar experiments [6] and calculations in Section 2.2).

Calculation of the Parameter G

Considering that the formation and focusing of the neutrino beam are influenced by a large number of independent or weakly dependent factors (angles of neutrino emission from π-meson decays, momentum spread of parent particles and π-mesons, multiple scattering in the target and focusing elements), it is reasonable to assume a Gaussian distribution for the neutrinos in the beam. Figure 8 provides a visual comparison of this model with a uniform distribution. The quantities r and R represent the linear size of the detector and the divergence of the muon neutrino beam focused to an angle θ, respectively.

Thus:

$$G = \frac{\int_0^r f(r) \cdot 2\pi r\, dr}{\int_0^R f(r) \cdot 2\pi r\, dr}, \tag{4}$$

where $f(r) = \frac{1}{\sqrt{2\pi}\sigma} e^{-\frac{r^2}{2\sigma^2}}$. Given that the distance to the detector is $L = 1350$ km and the beam divergence angle is $\theta = 0.01$ rad, the radius of the cone base is $R = L \cdot \theta = 13.5$ km, with a standard deviation of $\sigma = 4.6$ km. Additionally, knowing the effective detector area $S_{det} = 400\,\text{m}^2$, we estimate the linear size of the detector cross-section as $r \approx 11$ m. Calculating:

$$G = \frac{\int_0^r e^{-\frac{r^2}{2\sigma^2}} \cdot r\, dr}{\int_0^R e^{-\frac{r^2}{2\sigma^2}} \cdot r\, dr} = \frac{1 - e^{-\frac{r^2}{2\sigma^2}}}{1 - e^{-\frac{R^2}{2\sigma^2}}} = 2.9 \times 10^{-6} \tag{5}$$

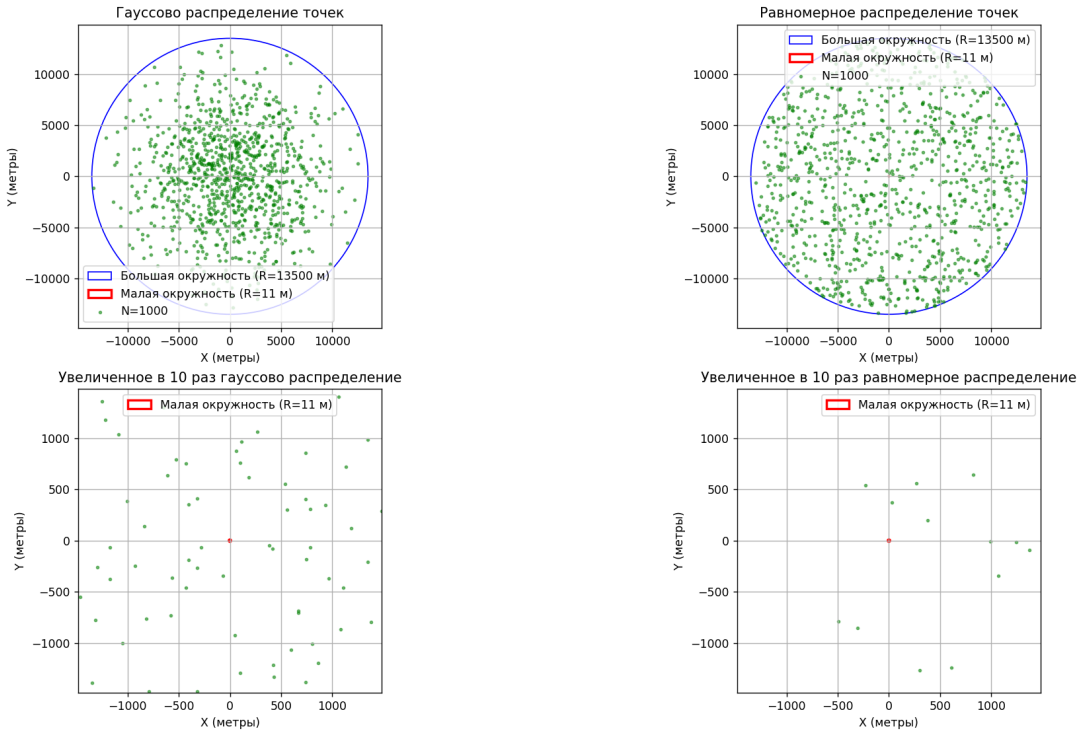

Figure 8: Visualization of the model of neutrino detection within the effective detector area for uniform and Gaussian-like distributions. The large blue circle represents the maximum divergence of the neutrino beam at a distance of 1350 km, and the small red circle represents the effective detector area.

Calculation of the Parameter k

As mentioned earlier, the coefficient k describes the efficiency of neutrino production, i.e., the ratio of the number of produced neutrinos to the total number of protons colliding with the graphite target. As a first approximation, we consider only the contribution of pions to the generation of the neutrino beam, with the decay probability of a π^+ meson into an antimuon and a muon neutrino being close to unity.

$\pi^+ \to \mu^+ + \nu_\mu$ (>99 %)

To proceed with further calculations, it is necessary to model the collision process of protons accelerated to 70 GeV with ^{12}C nuclei (graphite target), which was performed using the PYTHIA software. Below are histograms of the energy spectrum (Fig. 9) and multiplicity (Fig. 10) for π^+ mesons.

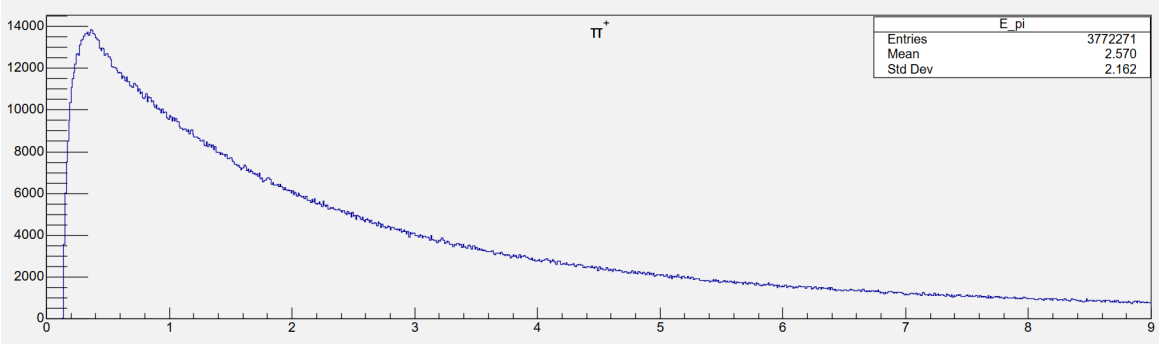

Figure 9: Energy spectrum of π^+ mesons produced from proton collisions with nuclei of the graphite target. The average value is 2.57 GeV.

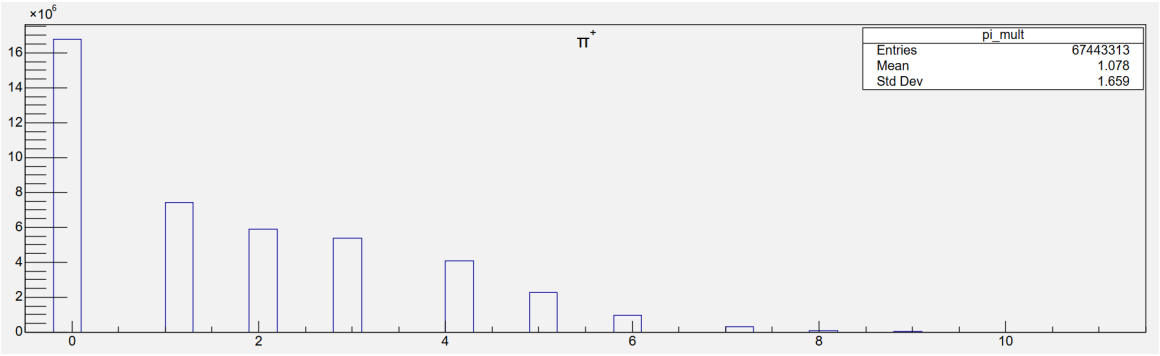

Figure 10: Multiplicity of π^+ mesons produced from proton collisions with nuclei of the graphite target. The average value is $M = 1.078$.

We consider the following model for generating the muon neutrino flux. Protons accelerated to 70 GeV collide with carbon nuclei (^{12}C) in a graphite rod (a cylinder 90 cm long and 2 cm in radius), partially inserted into the first horn. In the collision processes, pions are predominantly produced, which are then focused by the magnetic horn and directed into the decay channel. However, some pions are captured by the target nuclei or emitted at excessively large angles, making them insufficiently focused. Thus, we obtain the formula for estimating k:

$$k = M \times P_{esc} \times P_{angle} \tag{6}$$

where M is the multiplicity of pion production per proton, P_{esc} is the probability that a pion escapes the target (not captured by the target nuclei), and P_{angle} is the probability that a pion is emitted from the target at angles suitable for further capture by the horn.

The pion production multiplicity was estimated in Fig. 10, so we now need to evaluate the probabilities P_{esc} and P_{angle}. Let us start with the latter:

$$P_{angle} = \frac{1}{L} \times \int_0^L \frac{\int_0^{\theta_{max}(l)} \frac{dN}{d\theta}\, d\theta}{N_{total}}\, dl, \tag{7}$$

where $L = 90$ cm is the target length, N_{total} is the normalization to the total number of pion production events in the target,
$\theta_{max} = \arctan\left(\frac{L}{L-l} \times \tan(\alpha)\right)$ is the maximum angle at which a pion emitted at a distance $l \in [0; 90]$ cm from the start of the target is still captured by the magnetic field of the horn and directed into the decay pipe (α is the initial angle, taken as 2.5 degrees), and $\frac{dN}{d\theta}$ is the distribution of initial pion emission angles (histogram in Fig. 5).

Numerical integration yields the probability $\mathbf{P_{angle} = 0.395}$. However, it should be noted that this approximation assumes a uniform distribution of pion production probability, or equivalently, the probability of proton interaction with carbon nuclei, along the entire target length L. In the case of a non-uniform distribution, a lower value of P_{angle} is expected, as more pions would be produced closer to the start of the target, resulting in smaller acceptable emission angles for capture by the horn.

Now, let us evaluate P_{esc}. First, we need to determine the mean free path of π^+ mesons with an average energy of 2.57 GeV in the carbon target.

$$\lambda = \frac{1}{n \times \sigma}, \tag{8}$$

where n is the nuclear density of carbon in the target, and σ is the interaction cross-section of pions produced in the target with carbon.

For the nuclear density:

$$n = \frac{N_A \times \rho}{\mu} = \frac{6.022 \times 10^{23} \times 2.26}{12} \approx 1.13 \times 10^{23} \, \frac{1}{\text{cm}^3} \tag{9}$$

The cross-section was estimated using the GEANT4 software. The simulation accounted for inelastic interactions leading to the capture of produced pions by the target nuclei. For our purposes, we limit ourselves to an estimate at the average pion energy: $\sigma \approx 200$ mb (calculations are ongoing, this is a preliminary value). Hence:

$$\lambda = \frac{1}{1.13 \times 10^{23} \times 200 \times 10^{-27}} \approx 44 \, \text{cm} \tag{10}$$

We also estimate the probable distance traveled by a pion before a collision. With sufficient accuracy, we consider the most probable pion emission angle $\theta \approx 0.1$ rad at a target radius $R = 2$ cm:

$$\langle l \rangle = \frac{R}{\sin(\theta)} = \frac{2}{\sin(0.1)} \approx 20 \, \text{cm} \tag{11}$$

The process describing the frequency of pion interactions with target nuclei follows a Poisson distribution with mean $\mu = \frac{\langle l \rangle}{\lambda}$, thus:

$$P_{esc} = \frac{\mu^k \times e^{-\mu}}{k!} = \{k = 0\} = \exp\left(-\frac{\langle l \rangle}{\lambda}\right) = \exp\left(-\frac{20}{44}\right) \approx 0.63 \tag{12}$$

Taking all the above calculations into account, we finally obtain the value of the coefficient:

$$k = M \times P_{angle} \times P_{esc} = 1.078 \times 0.395 \times 0.63 \approx 0.268 \tag{13}$$

Calculation of the Upper Bound on the Number of Events per Year

Considering the previous sections, we obtain an estimate for the number of events detected per year:

$$n = \frac{N_p \times k \times G \times \sigma_\nu \times N_{nucl}}{S_{det}} \sim 10^4 \tag{14}$$

However, it should be noted that this value represents an upper bound and is highly idealized, serving primarily to assess the suitability of the considered system for the experiment. For more detailed modeling of the experiment, it is also necessary to: account for detector effects, model the horn system and target in detail, and consider the possibility of installing a near detector.

To increase the experiment's efficiency and the number of events in the far detector, the following options can be considered:

1) Increasing the accelerator power (up to 450 kW [2], which is five times higher than considered), thereby increasing the annual number of proton collisions with target nuclei.

2) Improving the efficiency of pion production from the target. For this purpose, alternative target materials, such as uranium or tungsten, could be considered. However, such a replacement complicates operation and imposes additional constraints.

3) Increasing the scintillator volume and the effective detector area, which would increase not only the effective detector cross-section but also the neutrino flux reaching the detector (considering the assumed model of neutrino distribution in the flux).

4 Accounting for Oscillations

Neutrinos produced in a specific flavor state (e.g., ν_e, ν_μ, ν_τ) can transform into other flavor states as they propagate through space. This phenomenon, called neutrino oscillations, indicates that neutrinos have non-zero mass, and their states are superpositions of mass eigenstates ν_i ($i = 1, 2, 3$) with different masses m_i. This fact goes beyond the Standard Model, making the study of neutrinos a key direction in the search for new physics.

The connection between flavor and mass states of neutrinos is described by the Pontecorvo–Maki–Nakagawa–Sakata (PMNS) mixing matrix. In the three-flavor model, this matrix is parameterized by three mixing angles (θ_{12}, θ_{13}, θ_{23}) and the CP-violation phase δ_{CP}. The oscillation probabilities depend on these parameters, as well as on the differences in the squares of the neutrino masses $\Delta m^2_{ij} = m^2_i - m^2_j$.

To date, most oscillation parameters have been measured with high precision. For example, the angle θ_{13} was determined in reactor experiments, and the parameters θ_{12} and Δm^2_{21} — in experiments with solar and reactor neutrinos. The values of all these parameters for further calculations are taken from article [8]. However, two fundamental questions remain open:

1. Neutrino mass hierarchy.

2. CP-invariance violation

Previously, we neglected oscillations when counting the number of events potentially registered in the Baksan detector. Now, we will account for neutrino oscillations to model the experiments:

1) Appearance of electron (anti)neutrinos: $P(\nu_\mu \to \nu_e)$

2) Disappearance of muon (anti)neutrinos: $P(\nu_\mu \to \nu_\mu)$

It should be noted that CP-violation cannot be observed in "disappearance" experiments.

When neutrinos pass through matter, significant changes in oscillation parameters are possible. Indeed, in this case, neutrinos interact with matter. All three types of neutrinos ν_e, ν_μ, ν_τ interact equally with electrons and nucleons in matter via the neutral weak current. Electron neutrinos ν_e additionally interact with electrons in matter via the charged weak current ($\nu_e + e^- \to e^- + \nu_e$). Significant changes in the interaction cross-sections of neutrinos with electrons and nucleons in matter are possible. This change will differ for ν_μ, ν_τ neutrinos and for electron neutrinos. As a result, the oscillation patterns for different flavors will differ.

Calculation of Probabilities in the Appearance Experiment

To plot the probabilities of muon neutrino oscillations to electron neutrinos (Fig. 11) in the three-flavor neutrino model, we will use an approximate formula typical for long-baseline accelerator experiments [7]:

$$\begin{aligned} P_{\mu e} = P(\nu_\mu \to \nu_e) \approx 4 s^2_{23} s^2_{13} c^2_{13} \frac{\sin^2(\Delta_{31} - aL)}{(\Delta_{31} - aL)^2} \Delta^2_{31} + \\ + 8 \frac{J}{\sin \delta_{CP}} \frac{\sin(\Delta_{31} - aL)}{(\Delta_{31} - aL)} \Delta_{31} \frac{\sin(aL)}{(aL)} \Delta_{21} \cos(\Delta_{31} + \delta_{CP}) + \\ + 4 s^2_{12} c^2_{12} c^2_{13} c^2_{23} \frac{\sin^2(aL)}{(aL)^2} \Delta^2_{21}, \end{aligned} \tag{15}$$

where $\Delta_{j1} \equiv \Delta m^2_{j1} L/4E$, $s_{ij} \equiv \sin\theta_{ij}$, $c_{ij} \equiv \cos\theta_{ij}$, and $J \equiv s_{23} c_{23} s^2_{13} c_{13} s_{12} c_{12} \sin\delta_{CP}$ is the Jarlskog invariant. The influence of the neutrino flux passing through the Earth's crust is accounted for in the parameter:

$$a \approx \frac{1}{3500\,\text{km}} \times \left(\frac{\rho}{2.84\,\frac{\text{g}}{\text{cm}^3}} \right), \tag{16}$$

where ρ is the density of matter along the flux path.

The general form of the matter coefficient in the considered approximation is as follows:

$$a = \frac{2EV}{\Delta_{31}},$$

The sign of the coefficient depends on the neutrino mass ordering: $A > 0$ for $\Delta_{31} > 0$ (NO — normal ordering) and $A < 0$ for $\Delta_{31} < 0$ (IO — inverted ordering). The potential V is due to the scattering of ν_e on electrons in the medium via charged currents. This type of interaction is characteristic of electron (anti)neutrinos. To calculate the oscillation probability $\nu_\mu \to \nu_e$ in the formula above, it is necessary to replace $\delta_{CP} \to -\delta_{CP}$ and $A \to -A$ ($V \to -V$). Thus, the probabilities of $\nu_\mu \to \nu_e$ and $\bar{\nu}_\mu \to \bar{\nu}_e$ oscillations depend on the sign of Δ_{31} — the neutrino mass hierarchy, the angle θ_{23} ($\theta_{23} < \pi/4$ or $\theta_{23} > \pi/4$), and the CP-violation phase. The amplitude of $\nu_\mu \to \nu_e$ ($\bar{\nu}_\mu \to \bar{\nu}_e$) oscillations will be maximum (minimum) for NO and $\delta_{CP} \approx -\pi/2$ and minimum (maximum) for IO and $\delta_{CP} \approx \pi/2$.

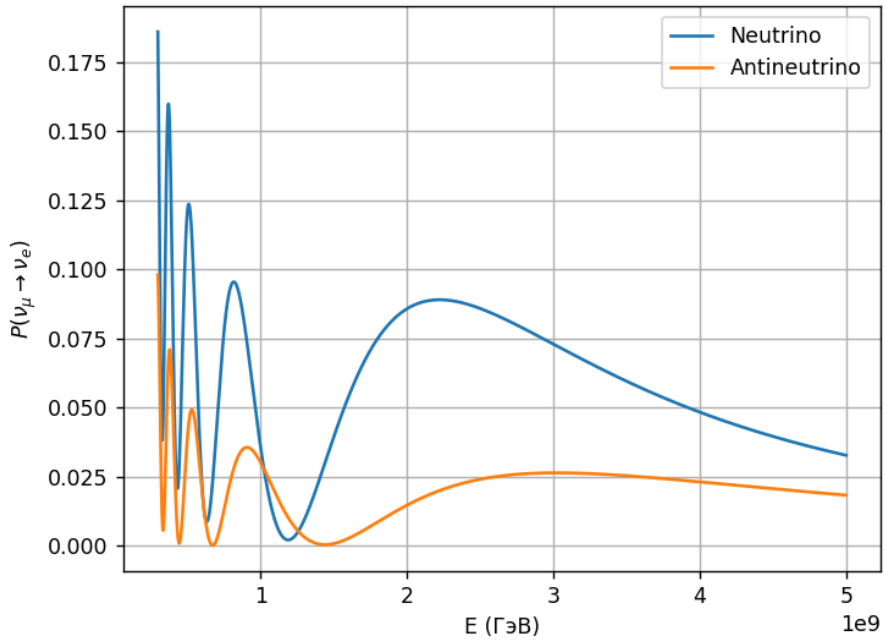

Figure 11: Plot of oscillation probabilities for neutrinos and antineutrinos in PtB.

Bi-probabilities are a tool for visualizing and analyzing neutrino oscillations, particularly in the context of determining the mass ordering and studying CP-violation in the leptonic sector. To plot bi-probabilities at energies of 2 GeV and 3 GeV, respectively (Figs. 12 and 13) for the PtB experiment, adjustments must be made to formula (14) when calculating antineutrino oscillation probabilities: $\delta_{CP} \to -\delta_{CP}$ and $(aL) \to -(aL)$. The neutrino–antineutrino asymmetry is used as a measure of CP-invariance violation.

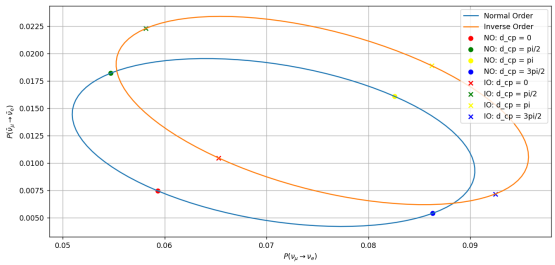

Figure 12: Bi-probability plot for PtB ($E_\nu = 2$ GeV).

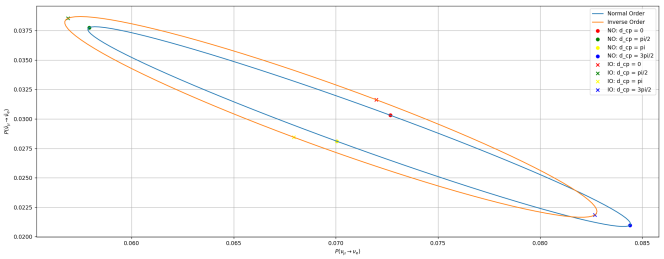

Figure 13: Bi-probability plot for PtB ($E_\nu = 3$ GeV).

Calculation of Probabilities in the Disappearance Experiment

In the case of $\nu_\mu(\bar{\nu}_\mu) \to \nu_\mu(\bar{\nu}_\mu)$ oscillations, matter effects are strongly suppressed [9], and the survival probability of muon (anti)neutrinos is well approximated by the expression:

$$P(\nu_\mu \to \nu_\mu) \approx 1 - \left(\cos^2\theta_{31}\sin^2 2\theta_{23} + \sin^2 2\theta_{13}\sin^4\theta_{23}\right)\sin^2\Delta_{31}, \tag{17}$$

where $\Delta_{31} = \Delta m^2_{31} L/E$, L is the experiment baseline, and E is the neutrino energy.

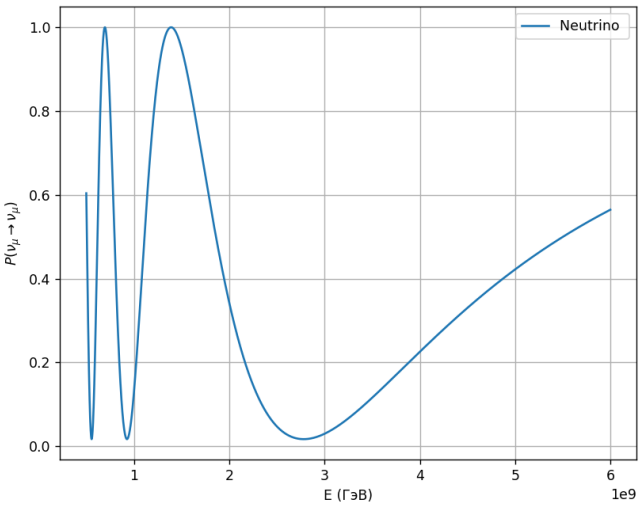

Figure 14: Plot of muon neutrino oscillation probabilities in PtB.

As follows from Fig. 14, the survival probability of muon neutrinos $P(\nu_\mu \to \nu_\mu)$ approaches 1 under certain conditions but never reaches 0 within the standard three-flavor model, given the known values of oscillation parameters. The value $P \approx 1$ occurs when two conditions are met:

1. The oscillation term vanishes:

$$\sin^2(\Delta_{31}) = 0 \quad \Rightarrow \quad \frac{\Delta m^2_{31} L}{4E} = k\pi \quad (k \in \mathbb{N}). \tag{18}$$

This corresponds to distances $L = k \cdot \frac{4\pi E}{\Delta m^2_{31}}$, where the phase difference between mass states is a multiple of 2π, and the neutrino returns to its initial state.

2. Neglecting small effects:

- The influence of Δm^2_{21} is extremely small for $\nu_\mu \to \nu_\mu$, so it can be neglected.
- In matter, the MSW effect for ν_μ is weak, so the contribution from the matter parameter is negligibly small.

Complete disappearance of the ν_μ component ($P = 0$) is impossible due to the non-zero angle θ_{13}. Even if $\theta_{23} = 45°$ (maximum mixing), terms remain in the formula that ensure a non-zero probability for the ν_μ state.

5 Building Spectra

To construct the neutrino spectra plots for this experiment, it is necessary to use estimates for $\sigma(E_\nu)$ (Fig. 7) and $\Phi(E_\nu)$ (Fig. 4). The spectra themselves will be constructed using the Global Neutrino Analysis (GNA) software.

Cross-Section of Muon Neutrino Interaction with Matter σ(E)

For the calculation of the cross-section spectrum, a model used in GENIE v3 was applied. Since the Baksan scintillator material is organic, primarily composed of carbon and hydrogen, the isoscalar target model is well-suited for describing the detector. To construct the cross-section spectrum plot, we will also rely on data from the CERN-SPS NOMAD collaboration experiments [10]. Thus, using the available data, we apply the spline interpolation method to approximate the dependence of the muon neutrino cross-section on their energy (Fig. 15).

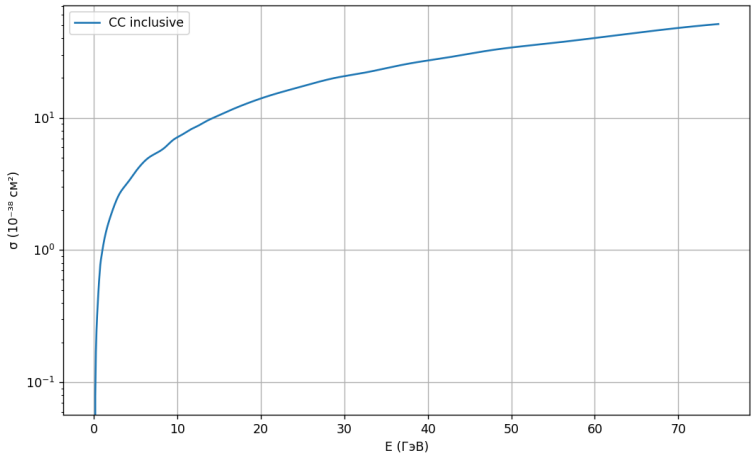

Figure 15: Cross-section of ν_μ interaction with isoscalar targets

Modeling the Muon Neutrino Flux in the PtB Experiment

Since we are considering an on-axis beam, the flux spectrum near the detector remains very broad, as shown, for example, in Fig. 16 at $\theta = 0$, where θ is the angle between the direction of the proton/pion flux and the neutrino flux. We observe that the neutrino spectrum at a non-zero angle is narrower and peaks at a lower energy due to the existence of a maximum possible neutrino energy for decays at a given angle relative to the parent pion's direction. The estimated on-axis flux spectrum for the PtB experiment is presented in Fig. 17.

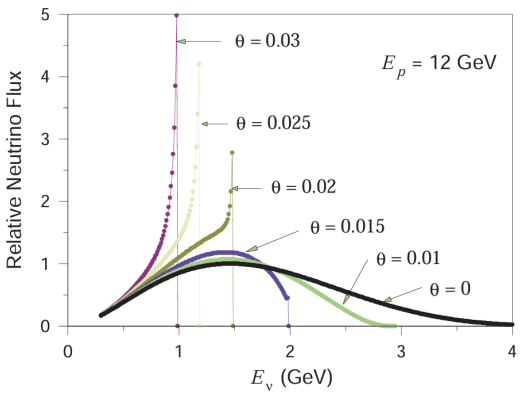

Figure 16: Muon neutrino flux spectrum for certain angles θ for protons with energy $E_p = 12\,\text{GeV}$. [3]

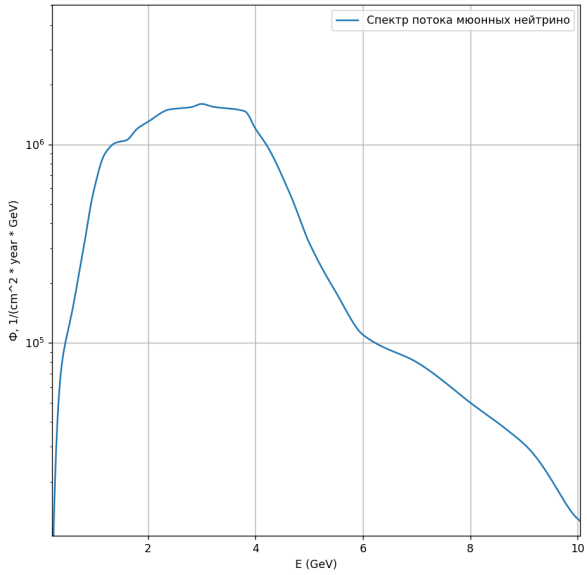

Figure 17: Energy spectrum of the muon neutrino flux without accounting for oscillations in the PtB experiment.

Spectrum of Event Rates for Electron and Muon Neutrinos Without Accounting for Detector Efficiency

From previous calculations, a data.txt file was created, in which cross-sections and fluxes were calculated with a step of 0.01 GeV in the energy range (0.05; 70) GeV. This file was then used to construct plots in the GNA software. The calculation formula for constructing annual spectra (Figs. 18, 19, 20) is given by:

$$\frac{dN}{dE} = \Phi(E) \times \sigma(E) \times N_{nucl} \times P_{osc}(E) \tag{19}$$

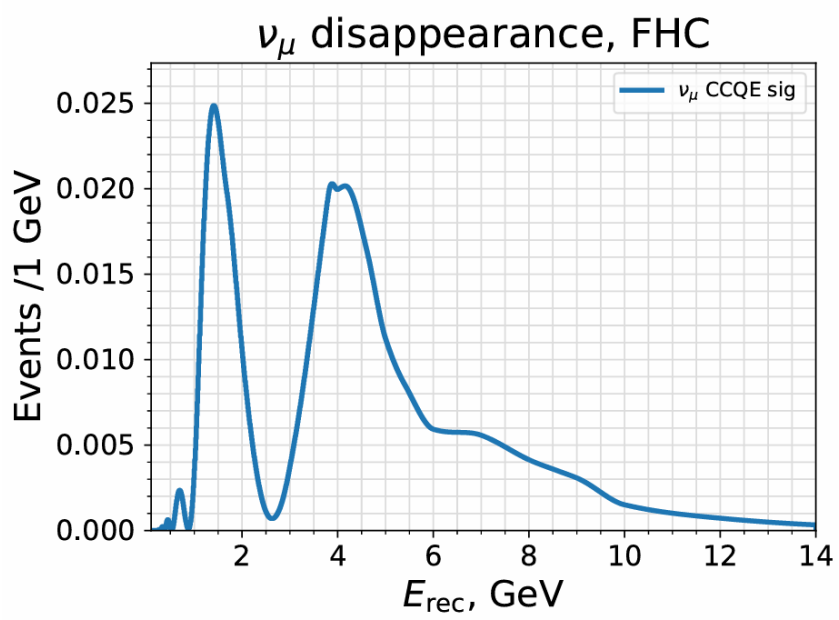

Figure 18: Annual event rate spectrum for $\nu_\mu \to \nu_\mu$ in the PtB experiment. The number of events per year is **7.94**.

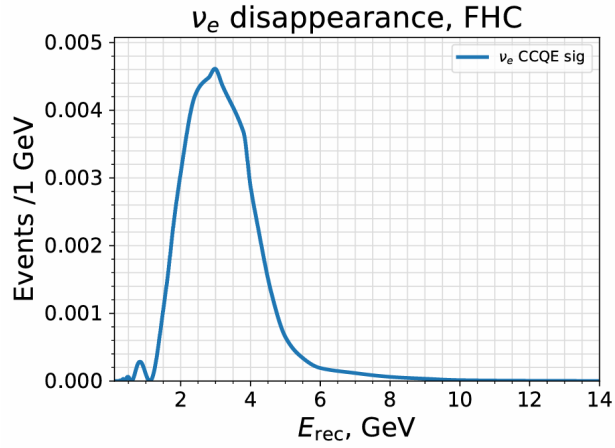

Figure 19: Annual event rate spectrum for $\nu_\mu \to \nu_e$ in the PtB experiment. The number of events per year is **1.17**.

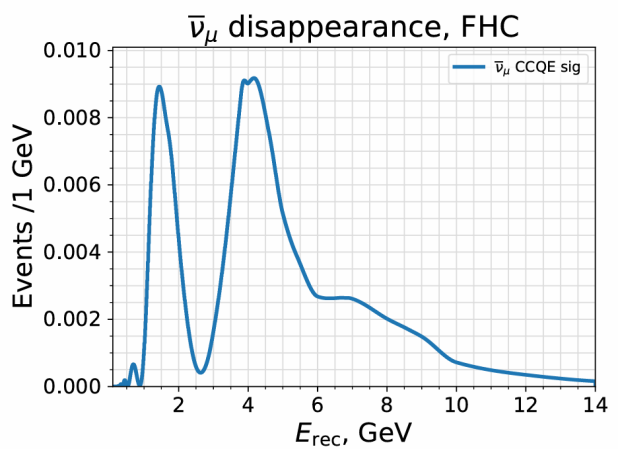

Figure 20: Annual event rate spectrum for $\bar{\nu_\mu} \to \bar{\nu_\mu}$ in the PtB experiment. The number of events per year is **3.47**.

6 Estimation of Sensitivity in Measuring Oscillation Parameters in the PtB Experiment

In this section, all calculations and modeling will be performed at an exposure of 10 kiloton-years, which is approximately 30 times greater than the current statistics, allowing for a more accurate assessment of the experiment's sensitivity to measuring certain oscillation parameters. The development of a prototype for such a potential Baksan Large Neutrino Telescope (BLNT) is discussed in the dissertation [11].

Figures 21 and 22 show the PtB sensitivity to the phase δ_{CP} for normal and inverted neutrino mass hierarchies. The simulation was conducted for a period of 1 year.

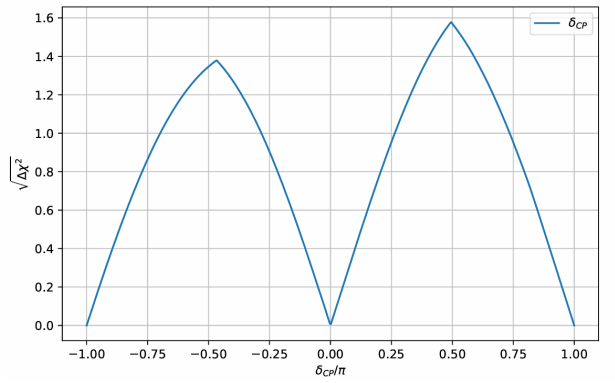

Figure 21: PtB sensitivity to the phase δ_{CP} for normal mass hierarchy

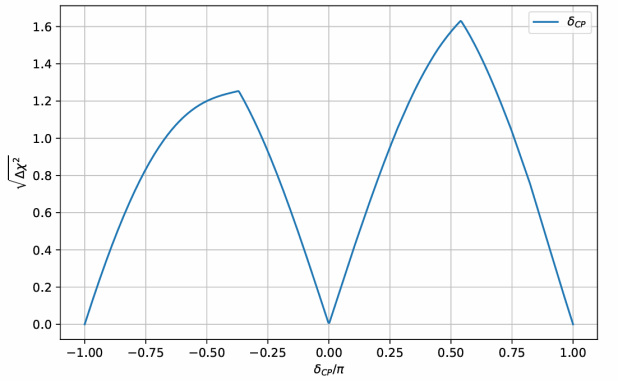

Figure 22: PtB sensitivity to the phase δ_{CP} for inverted mass hierarchy

Figures 23 and 24 depict plots illustrating the PtB sensitivity to the neutrino mass hierarchy. To determine the neutrino mass hierarchy at a significance level of 5 σ, the experiment in the described configuration would approximately require 4 years of data collection.

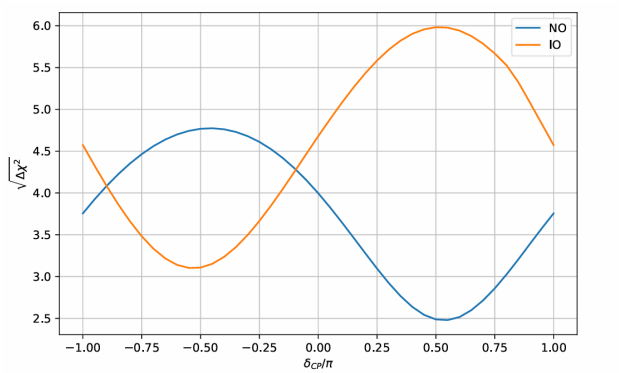

Figure 23: PtB sensitivity to the mass hierarchy (exposure of 10 kiloton-years)

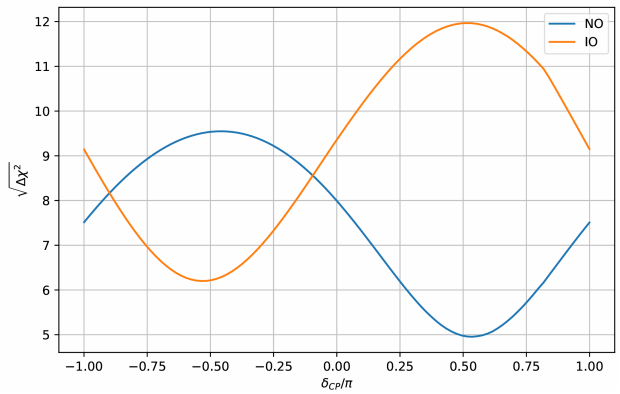

Figure 24: PtB sensitivity to the mass hierarchy (exposure of 40 kiloton-years)

7 Conclusion

The hypothetical Protvino-to-Baksan experiment modeled in this work is currently of limited suitability, primarily due to the small detector volume and certain technical challenges associated with directing the neutrino beam from the U-70 accelerator. However, considering the potential for installing or upgrading the detector, the experiment becomes potentially valuable and promising.

Given that the detector and accelerator locations were not specifically chosen for neutrino oscillation studies, the distance between the detector and the accelerator, as well as the neutrino energy, are not entirely optimal. For example, the PtB sensitivity to measuring the phase δ_{CP} is low. However, the experiment's sensitivity to the neutrino mass hierarchy, combined with possible configuration improvements, could yield results at a 5σ confidence level within 4 years.

Acknowledgments

I would like to express my deep gratitude to Lyudmila Kolupaeva, Anna Stepanova, and Anastasia Kalitkina for their assistance in writing this work and for creating a wonderful working atmosphere. Special thanks to Anna and Anastasia for their excellent consultations on the GNA software.

References

[1] "Study of Neutrino Oscillations Using Neutrino Beams from the U-70 Accelerator Complex" by V.I. Garkusha, F.N. Novoskol'tseva, and A.A. Sokolov
(http://web.ihep.su/library/pubs/prep2015/ps/2015-5.pdf)
[2] Letter of Interest for a Neutrino Beam from Protvino to KM3NeT/ORCA
(https://arxiv.org/abs/1902.06083)
[3] An Off-Axis Neutrino Beam, Kirk T McDonald
(https://arxiv.org/abs/hep-ex/0111033)
[4] https://www.inr.ru/rus/bno/lbpst.html
[5] Neutrino-Nucleon Cross-Section Model Tuning in GENIE v3
(https://arxiv.org/pdf/2104.09179)
[6] Neutrino Flux Predictions for the NuMI Beam
(https://arxiv.org/pdf/1607.00704)
[7] The fate of hints: updated global analysis of three-flavor neutrino oscillations
(https://arxiv.org/pdf/2007.14792)
[8] Back to (Mass-)Square(d) One: The Neutrino Mass Ordering in Light of Recent Data
(https://arxiv.org/pdf/2007.08526)
[9] Results of Neutrino Experiments T2K and NOvA: Neutrino Mass Ordering and CP-Symmetry A.V. Butkevich
(`http://www.jetp.ras.ru/cgi-bin/dn/r_161_0515.pdf`)
[10] A Precise Measurement of the Muon Neutrino-Nucleon Inclusive Charged Current Cross-Section off an Isoscalar Target
(https://www.hepdata.net/record/ins767013)
[11] Development and Creation of a Half-Ton Prototype of the Baksan Large Neutrino Telescope, Nikita Andreevich Ushakov
(https://www.inr.ru/rus/referat/uschakov/dis.pdf)